Chapter 31

Functionalized Vesicles by Microfluidic Device

Derek Vallejo, Shih-Hui Lee, and Abraham Lee

Abstract

In recent years, lipid vesicles have become popular vehicles for the creation of biosensors. Vesicles can hold reaction components within a selective permeable membrane that provides an ideal environment for membrane protein biosensing elements. The lipid bilayer allows a protein to retain its native structure and function, and the membrane fluidity can allow for conformational changes and physiological interactions with target analytes. Here, we present two methods for the production of giant unilamellar vesicles (GUVs) within a microfluidic device that can be used as the basis for a biosensor. The vesicles are produced from water-in-oil-in-water (W/O/W) double emulsion templates using a nonvolatile oil phase. To create the GUVs, the oil can be removed via extraction with ethanol, or by altering the interfacial tension between the oil and carrier solution causing the oil to retract into a cap on one side of the structure, leaving behind an exposed lipid bilayer. Methods to integrate sensing elements and membrane protein pores onto the vesicles are also introduced in this work.

Key words Biosensor, Solvent extraction, Dewetting, Giant unilamellar vesicle, Artificial cell, Microfluidics

1 Introduction

A biosensor is an analytical tool that utilizes a biologically derived recognition element to detect an analyte of interest. The biological recognition element is the key to biosensor function and specificity, as the inherent advantage of a biosensor is to utilize the incredibly specific interaction of the biorecognition element with the analyte of interest. In turn, various substances and organisms can be detected in vital environmental resources (i.e., drinking water) or biological systems, with incredible specificity.

The interaction of the analyte with the bio-recognition element produces a physical or chemical change that is then converted by a transducer into an electrical signal proportional to the concentration of analyte in the sample. The biorecognition element is commonly an enzyme or protein [1], or antibody [2], but oligonucleotides [3], whole cells [4, 5], and organelles [6, 7] have also

Ben Prickril and Avraham Rasooly (eds.), *Biosensors and Biodetection: Methods and Protocols, Volume 2: Electrochemical, Bioelectronic, Piezoelectric, Cellular and Molecular Biosensors*, Methods in Molecular Biology, vol. 1572,
DOI 10.1007/978-1-4939-6911-1_31,

been used. In most cases, the biorecognition element is placed in direct physical contact with the transducing element [8]. The nature of the physical or chemical signal passed to the transducer can be electrochemical [9, 10], optical (fluorescent or colorimetric) [1, 11], calorimetric [12–14], or piezoelectric [15, 16], among others [17, 18]. While the biorecognition element allows for biosensors to have incredible specificity, it traditionally falls on the transducer to amplify the signal to increase the sensitivity of the system, and the degree and quality of this amplification will be limited by the particular transducer [19].

The sensing mechanism for a biosensor can take many forms: for example, the biosensor can utilize an enzyme that will initiate a biochemical reaction in response to an analyte binding event or a protein will undergo a conformation change when bound to the target analyte. In nature, cells sense their environment through a signaling cascade of multiple reactions that allow for highly efficient amplification [20]. For this reason, there has been an interest in using vesicles as biosensors for their ability to encapsulate biological reaction components. The very nature of the reaction can be one that involves signal amplification, such that the signal can be pre-amplified before reaching the transducer, or the vesicle can itself act as the transducer, further simplifying the system. By placing the components of the biochemical reaction within a small, confined volume, the concentration of product molecules can increase to a detectable level much more rapidly, and with much less analyte, than in a larger, bulk solutions. The use of an enzyme and a biochemical reaction scheme in a biosensor platform also means that a single molecule of analyte can initiate multiple reaction events, allowing for tremendous signal amplification and paving the way the for single molecule detection. Such technology can negate the need for analyte pre-enrichment above a specific detection threshold, as is still the case with many traditional detection platforms (PCR, Elisa, etc.) [21]. Placement within a physical boundary also protects the reaction components from contamination, allows the system to be deployable into sensitive, biological environments, and provides a platform for the placement of the sensing elements. Natural cells contain the ideal physical boundary between their interiors and the external environment, the lipid bilayer, which can be functionalized to meet a variety of demands and tasks. Over the last few decades, many biosensing platforms have utilized either planar or enclosed lipid bilayers, or their synthetic, biomimetic equivalents [22, 23]. With a membrane, the biorecognition element can either be enclosed within the vesicle, embedded within the membrane itself, or conjugated to the membrane surface. The biomimetic nature of lipid vesicles provides the ideal environment to stabilize and maintain the activity of proteins and enzymes for analyte detection and their inherent biocompatibility allows for them to be deployed in many biological

environments. The ease with which vesicles can be modified and functionalized also makes them compatible with many of the current sensor technologies mentioned previously and opens the possibility for multi-target sensing.

Enzymatic reaction events have been utilized in biosensor applications [24, 25], and with the design of artificial organelles, such reactions have been contained within vesicles and polymersomes [26–28]. While many artificial organelles are designed with the therapeutic intent to correct cellular function or introduce novel biochemical functions into established cells, the application to biosensing cannot be overlooked. For membrane permeable analytes, the design of the biosensor is simplified, in that there is no need for any active components to be in, or conjugated to, the membrane and all the sensing and reaction components can be entirely contained within the vesicle interior, where the result of the reaction releases a fluorescent signal that can be correlated to the concentration of analyte [29]. For example, Ben-Haim et al. demonstrated that enzymatic activity could be maintained within vesicles by encapsulating trypsin and using it to cleave the membrane permeable BZiPAR (bis-(CBZ-Ile-Pro-Arg)-R110, a Rhodamine 110 peptide substrate), releasing green fluorescent Rhodamine 110 [29]. Enzymatic cascades are also possible within vesicle structures, where different vesicles can contain different steps to an enzymatic cascade reaction, leading to the plausibility of compartmentalized, sequential reaction steps within a single structure. Such a scheme was demonstrated by encapsulating horseradish peroxidase (HRP) and glucose oxidase (GOx) in separate polymersomes to detect glucose [26]. After GOx converts glucose to into gluconolactone and H_2O_2, the membrane permeable H_2O_2 diffuses into solution and enters the polymersomes containing HRP and 2,2′-azino-bis(3-ethylbenzthiazoline-6-sulfonic acid) (ABTS), where the resultant reaction produces the ABTS radical cation ($ABTS^{*+}$). This reaction was also realized in a single structure with an additional extra step where membrane bound Candida antarctica lipase B (CalB) converts 1,2,3,4-tetra-*O*-acetyl-b-glucopyranose (GAc4) to glucose [27]. The polymersome biosensors that contained these reaction components were formulated to be naturally permeable to glucose so it could pass through the membrane and initiate the remainder of the reaction cascade in the interior. Channels imbedded in the membrane can also be utilized in vesicle biosensors as electrochemical detection schemes [30], or to allow the passage of membrane impermeable analytes to internal reaction components [1, 28]. With cascade events, amplification can be achieved in this format as well.

Vesicles have also been designed to be responsive to the environment by causing a structural change in the molecules that make up the membrane. Vesicles produced from polydiacetylene (PDA) lipids are very popular in this regard for use in colorimetric assays, as

they will undergo a rapid color change that is visible to the naked eye in response to various environmental stimuli, including pH, temperature, and exposure to a variety of molecules, peptides, and solvents [31]. For biosensor applications, biorecognition elements can be conjugated to the PDA vesicle membrane, and binding of analytes will cause a sharp color change, the degree of which is proportional to the concentration of analyte in the sample [32–34]. Although PDA vesicles are generally very stable, their production cost is currently prohibitive to widespread commercialization and they can suffer from issue with specificity, as they are naturally responsive to a wide range of stimuli.

Other effective strategies also exist to realize amplification with the use of vesicle that makes use of their mass and surface-to-volume ratio. For one, they can be used to encapsulate high concentrations of signaling molecules to increase the sensitivity of various types of immunoassays [35]. Antibodies specific to the analyte in question are immobilized to a surface and the vesicles can either be tagged with the analyte and compete with free analyte to bind with the immobilized antibodies (competitive immunoassay) or vesicles can be tagged with antibodies and bind to the analyte-immobilized antibody complex (sandwich immunoassay). In this way, a large concentration of signaling molecules can be associated with a single binding event, and analysis can be accomplished through the localization of dye containing vesicles for colorimetric [36–38] and fluorescent [39, 40] assays, release or production of ions for electrochemical signaling [35], and the release of chemiluminescent substrates for chemiluminescence assays [41] (*see* **Note 1**). The extra mass and size provided by vesicles relative to the analyte being detected is another use of vesicles for signal amplification. With surface plasma resonance (SPR) sensors, vesicles can be used in sandwich immunoassays to amplify the degree of SPR shift measured by the detector [42]. Vesicles can also enhance the sensitivity of quartz microbalances (QCM) [43, 44]. Quartz microbalances measure the mass of absorbed material based on its oscillation frequency, and this mass can be increased significantly with the attachment of a vesicle to each bound analyte on the microbalance. Theoretically, however, any nano- or micro-particle with a modifiable surface can accomplish the same effect as vesicles with respect to SPR and QCM.

With all the talk about the utility of vesicles for biosensor applications, there has yet to be wide spread adoption of vesicle based biosensors. A major bottleneck is their inherent fragility and short-shelf life, where fusion and lipid hydrolysis remain to be the most common culprits of population degradation. Long-term storage of a few months to more than a year will be a requirement of any biosensor kit utilized in the public domain. While freeze drying is a popular means of storage, this has not been successfully demonstrated with vesicles that are immobilized to surfaces and rehydration efficiency could potentially be a challenge [45].

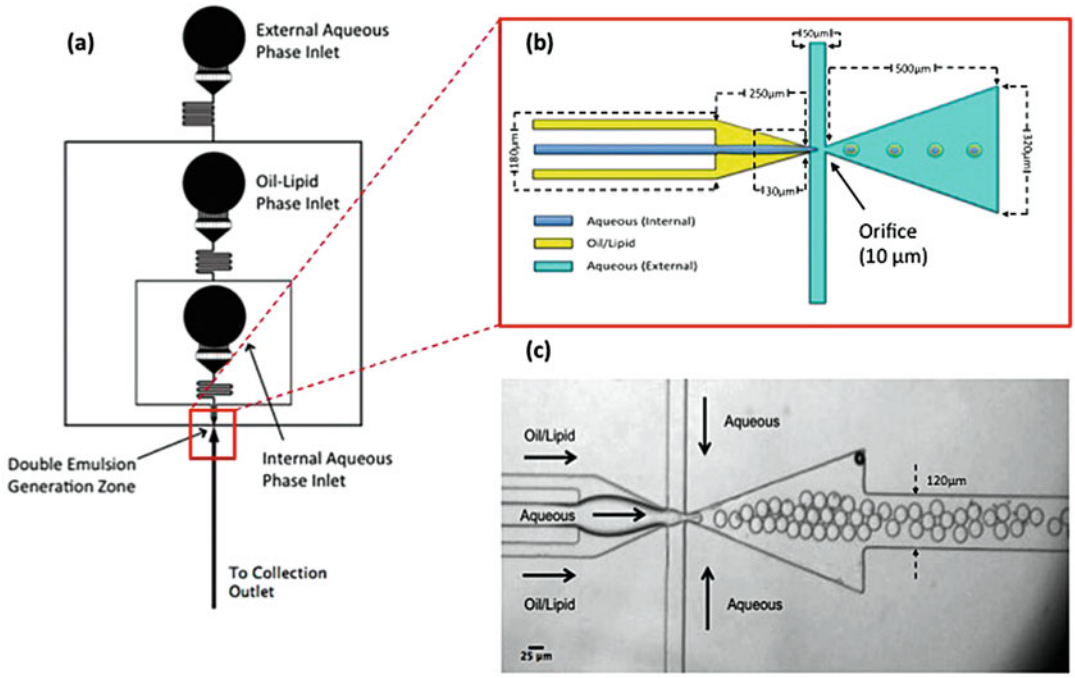

Fig. 1 Schematic and microscopic images of one-step double emulsion device and double emulsion generation. (**a**) Schematic of device design used for double emulsion production. (**b**) Close-up of double emulsion generation zone. Aqueous channels are 50 μm wide unless otherwise specified. Oil channels are 30 μm wide. (**c**) Microscopic image of double emulsion generation zone and double emulsion production

In this work, we report on two methods to create GUVs from microfluidically generated double emulsion templates that are suitable for long-term storage in an aqueous environment. Microfluidic methods offer the advantage of precise control over the size and lamellarity of the resultant vesicle population, and greatly increase the encapsulation efficiency over bulk methods [46, 47] (*see* **Note 2**). For both methods, W/O/W double emulsion precursors are formed within a single junction, co-focusing microfluidic device, as illustrated in Fig. 1. The oil phase consists of oleic acid with dissolved lipids. In the first method, the double emulsions are placed in an electrolyte solution whereby an increase in interfacial tension between the oil and external water phase causes the oil layer to undergo a dewetting process [48], forming a lipid bilayer and collecting as a "cap" on one side of the vesicle (Fig. 2). In the second method, the double emulsions are collected in a solution of 14% ethanol, whereby the oleic acid is extracted out by the ethanol solution to form a lipid bilayer over the course of 15 h, as described previously [49]. The GUVs produced from these methods can be used as a basis for future biosensing technologies and applications. We also present methods to integrate recognition elements on the vesicle surface and insert melittin to create a permeable channel for penetrating analytes.

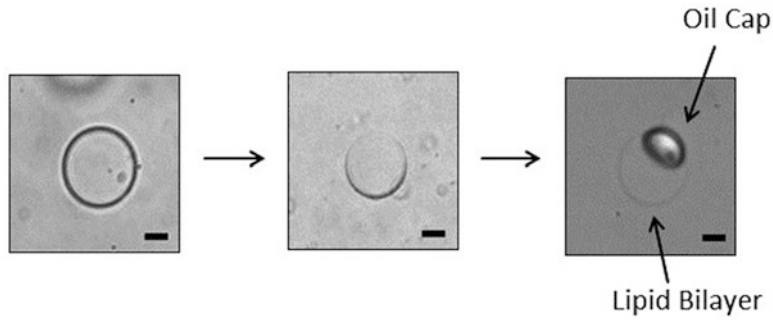

Fig. 2 Brigh-field microscopic images of the dewetting process. Process is from *left-to-right*. Upon exposure to increased interfacial tension from electrolytes, the oil in the double emulsion begins to accumulate to one side, causing a local thinning of the oil shell and an increase in the depletion force in that area. The lipid tails can then force out the excess oil and form a bilayer. Scale bar is 12 μm

2 Materials

2.1 SU-8 Master Mold Fabrication

1. Cleanroom facility (Class 1000 or greater).
2. 3 inch silicone wafer (Polishing Cooperation of America).
3. SU-8 photoresist (2025 or 2050, MicroChem).
4. 2% (v/v) hydrofluoric acid (HF). Solution is made by mixing 480 ml of water with 20 ml HF (49%). Protective eyewear, neoprene or thick nitrile gloves, and a neoprene apron must be worn while handling HF.
5. Photo Resist Spin Coater (Laurell Technologies).
6. UV Flood Exposure System (AB&M).
7. Transparency Mask (20,000 dpi, CAD/Art Services, Brandon, OR). The device design was drawn in AutoCAD (AutoDesk) and exported to Adobe Illustrator (Adobe) .esp format for printing.
8. 5 × 5 in. transparent glass or quartz sheet.
9. Hot plate.
10. Isopropyl alcohol (IPA, 99.9%).
11. Acetone (99.9%).
12. SU-8 developer (MicroChem).

2.2 Microfluidic Device Fabrication

1. Unidirectional flow tabletop workstation (TT-4830, Envirco Corporation, Albuquerque, NM).
2. Polydimethylsiloxane (PDMS) base and curing agent (Sylgard 184, Dow Corning).
3. Petri dish (100 mm × 15 mm, PD-3561, Phenix Research Products).

4. Harrick Air Plasma Cleaner (Harrick Plasma).
5. KJLC 205 Series Thermocouple Gauge Controller (Kurt J. Lesker Company).
6. Trivac D2,5 E Vaccum Pump (Oerlikon Leybold Vacuum, Product# 140002).
7. Compressed nitrogen gas tank (Airgas).
8. Spray gun (Furon®).
9. Biopsy punch (Integra™ Miltex®).
10. Vacuum/degassing chamber.
11. Oven (65 °C and 120 °C).
12. Light duty tissue wipes (One-Ply White Wipers, 4.5 × 8.3 in., VWR).
13. Standard glass microscope slide (Corning).
14. Scalpel (Staninless #3 scalpel holder and surgical blade No. 11, Feather).
15. 1 ml syringe (Norm-Ject®).

2.3 Imaging

1. Inverted microscope (TC2000-S, Nikon).
2. High speed camera (V310 Phantom, Vision Research) and associated software.
3. Compatible PC.

2.4 Fluid Pumping System

1. SMC ITV0011-2UMS digital regulator (Automation Distribution) and associated LabVIEW Software.
2. DC regulated power supply (1670A, BK Precision).
3. USB DAQ (×2, National Instruments).
4. Pressure supply (House air or tank).
5. Pressure regulator (Swagelok).
6. Tygon tubing (0.02in ID, 0.06in OD, AAD02103-CP, Cole-Parmer).
7. 2.0 ml freestanding screwcap tube (SCS020TF, Phenix Research Products).
8. 23 G ×1 needles ((0.6 mm × 25 mm, BD Precision™ Glide Needle).

2.5 Working Solutions

1. Internal Solution—5% solution of Pluronic F68, diluted with DI water from 10% Pluronic F68 (Sigma-Aldrich), and 250 mM sucrose (Fisher Scientific).
2. Middle Solution—10 mg/ml of DOPC (1,2-dioleoyl-sn-glycero-3-phosphocholine, Avanti Polar Lipids) and 5 mg/ml cholesterol (Avocado Research Chemicals, Ltd) dissolved in oleic acid (Fisher Scientific). This solution can be modified to

contain other lipids for surface conjugation of sensing elements, and will be referenced in the text.

(a) Covalently Bonded Amine Reaction: Add 10% molar ratio of DSPE-PEG(2000) Cyanur (Avanti Polar Lipids) to DOPC in middle solution.

(b) Biotin–Avidin Interaction: Add 1–10% molar ratio biotinylated lipid (DSPE-PEG(2000) Biotin, Avanti Polar Lipids) to DOPC in middle solution.

3. External Solution (Method 1)—2 parts (v/v) pluronic F68 (10% solution, Sigma-Aldrich), 1 (v/v) part glycerol (EMD Biosciences), and either 125 mM NaCl (Fisher Scientific) or 250 mM sucrose.
4. External Solution (Method 2)—1 part ethanol, 1 part glycerol, 1 part water, 4 parts 10% pluronic F68.
5. Storage Solution (Method 1)—0.5% pluronic F68 in 250 mM sucrose solution.
6. 0.4 and 0.1% (w/w) solutions of PVA (polyvinyl alcohol, average MW 30,000–70,000, 87%–90% hydrolyzed, Sigma-Aldrich).
7. 1% (v/v) Teflon® AF (DuPont™) in Fluorinert™ FC-43 (3 M™).

3 Experimental Setup and Methods

3.1 Creation of SU-8 Master Mold

The master mold is fabricated using standard UV photolithography techniques [50, 51], following the MicroChem protocols for SU-8 to achieve the desired feature height. The protocol is briefly described below for 40 μm high features. An external vendor prints the transparency mask via high-resolution printer at 20,000 dpi. The mask can produce ten devices on a single wafer and is printed such that the channel features are transparent on a black background (Fig. 3). **Steps 1–8** below need to be completed in a Class 1000 (or greater) cleanroom facility to ensure a dust-free master mold.

1. In a chemical fume hood, submerge the silicone wafer in 2% (v/v) HF solution for 15s, wash with water, and allow to dry at 120 °C for 20 min. Always wear proper personal protective equipment (PPE) when handling HF solutions and employ the buddy system. Do not use glass containers for HF.
2. Spin coat SU-8 2050 photoresist onto the silicon wafer. Spin at 500 rpm ($21.3 \times g$) for 10s to ensure even spreading, then ramp up to 4000 rpm ($1363 \times g$) to achieve a 40 μm feature height.
3. Soft bake the wafer at 65 °C for 3 min and 95 °C for 6 min.

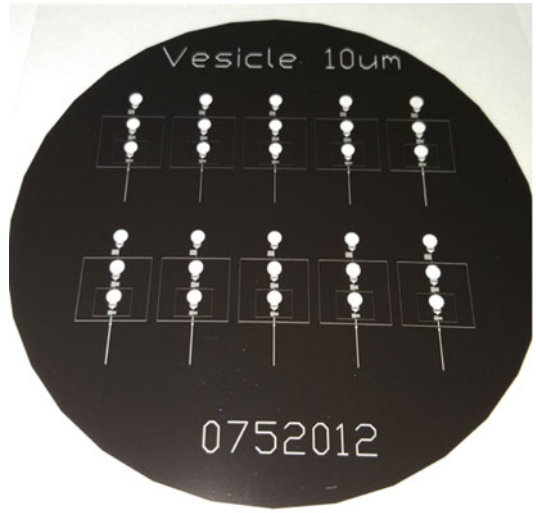

Fig. 3 Photograph of transparency mask. Each mask can produce ten individual devices

4. Remove silicon wafer from oven or hotplate and place in the UV flood exposure lamp. Place and center the transparency mask on top of the wafer and place a 5in ×5in glass sheet on top of the transparency mask to prevent light leakage.
5. Expose the wafer to 160 mJ/cm^2. To calculate the time needed to expose the wafer to UV radiation, divide the exposure energy by the power output of the UV lamp (mW/cm^2).
6. Bake the wafer at 65 °C for 1 min and 95 °C for 6 min.
7. Place the wafer in SU-8 developer for 5 min. While the wafer is submerged in developer, move the container in small infinity motions to ensure complete removal of undeveloped photoresist (more important for high aspect ratio features). A sonicator can also be used for high aspect ratios, but the development time should be reduced accordingly.
8. Wash wafer with excess SU-8 developer, followed by IPA.
9. Hard bake the patterned wafer at 150–200 °C for 5 min.
10. Spin coat with 1% (v/v) Teflon® AF in Fluorinert™ FC-43 at 3000 rpm (768 × *g*) for 30 s. Cover entire wafer with a thin layer of solution before running spinner.
11. Place wafer in 120 °C oven for 1 min.
12. Store wafer in a dry, dust-free environment. The wafer can be reused for many years.

1. The plasma chamber is set up in a laminar flow hood to prevent the inflow of dust and debris. An image of the setup can be seen in Fig. 4.

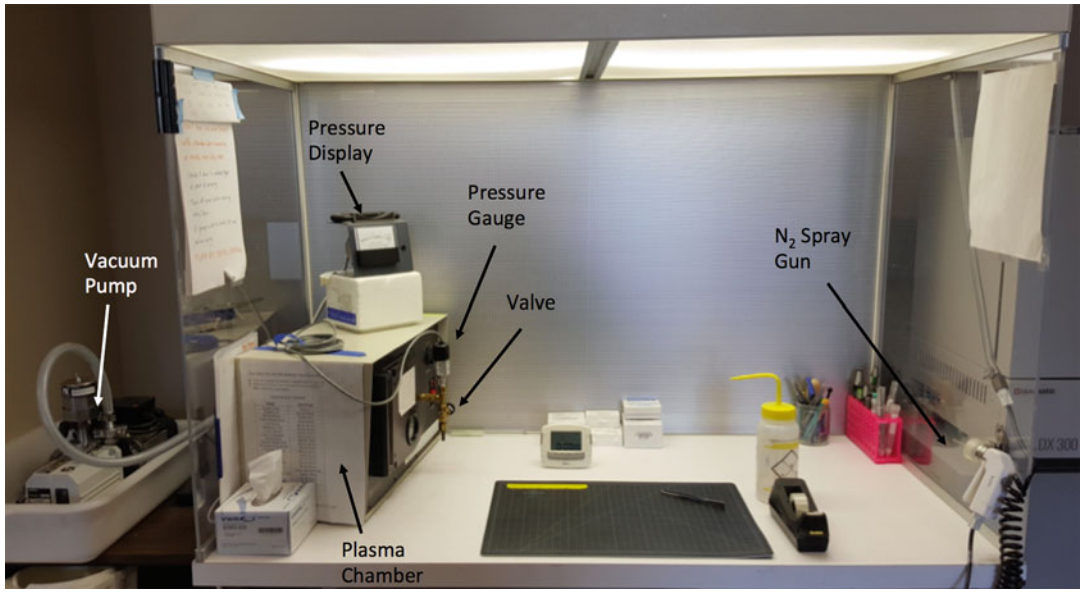

Fig. 4 Photograph of plasma chamber setup

3.2 Microfluidic Device Fabrication

3.2.1 Plasma Chamber Setup

2. The rear of the plasma chamber is connected to the vacuum pump using 3/8 in ID reinforced tubing and tightened in place with hose clamps.
3. The perpendicular portion of a brass T-junction pipe is secured to the front door of the plasma chamber. The pressure gauge is connected to one end of the T-junction pipe and a valve to the other. The valve is used to control the pressure inside the plasma chamber during operation.
4. A scalpel, N_2 spray gun, tape, punches, lint-free tissue wipes, IPA, and glass slides are kept close by to aid in PDMS device fabrication.

3.2.2 PDMS Fabrication Methods

1. Place the wafer in a petri dish, and fill it with 20–25 g of PDMS pre-polymer base–curing agent mixture. The PDMS should be mixed at a 10:1 (w/w) ratio of base to curing agent until it has a milky, opaque appearance.
2. Pour the PDMS into the petri dish over the wafer and degas in a vacuum chamber for at least 30 min or until PDMS is transparent and no bubbles remain.
3. Place in a 65 °C to cure for at least 4 h.
4. Once cured, cut out the desired number of devices with a surgical scalpel or similarly sharp blade, cutting around the devices to not ruin any of the SU-8 features.
5. With tweezers, pull up a corner of the cut section and begin to peel off the PDMS device.

6. Use the biopsy punch to produce holes for the fluid inlets and outlets. Inlets are labeled in Fig. 1 and can be seen as the large circles in the transparency mask (Fig. 3). An outlet hole should be punched at the end of the straight channel labeled "To Collection Outlet" in Fig. 1.
7. Clean off any excess dust using scotch tape and an N_2 spray gun.
8. Place the device, channel side up, inside the plasma chamber.
9. Clean a glass slide with IPA (wipe with tissue and spray clean with N_2)
10. Place cleaned slide in plasma chamber.
11. Close plasma chamber and seal valve. Turn on pump and allow to pump down past 300 mTorr. Adjust valve to maintain pressure at 300 mTorr. Turn on plasma.
12. Treat device in air plasma for 60–90 s (device has a surface area slight smaller than glass slide. Larger devices require longer treatment times).
13. After the set time has passed, turn off the plasma, then the pump, and remove device once pressure has equalized.
14. Immediately place the device, channel side down, on the surface of the glass slide that has been exposed to the plasma. Push out any air bubble by pressing down with tweezers or similar object. The air plasma removes the methyl groups from the PDMS surface and replaces them with silanol (SiOH) groups (rendering the surface hydrophilic). The silanol groups will form a covalent bond with the silica (SiO_2) groups on the glass slide to form a siloxane (Si-O-Si) bond, permanently sealing the PDMS to the glass slide [50].

3.3 Surface Treatment

Since PDMS is naturally hydrophobic, to successfully form W/O/W double emulsions, the channel carrying the continuous phase must be hydrophilic to ensure that the oil phase does not interact with the walls of the device. To accomplish this, the walls of the continuous phase channel are treated with a 0.4% (w/w) solution of PVA, as described by Teh et al. [49]. The setup can be seen in Fig. 5.

1. Connect the outlet of the device to a vacuum line.
2. Place 5–10 μl of a 0.4% (w/w) solution of PVA into the continuous phase inlet.
3. After 15–30 s place 5–10 μl of a 0.1%(w/w) solution of PVA into the continuous phase inlet. This step is to clean any excess PVA that may have accumulated in the droplet generation region.
4. Leave the device connected to the vacuum for at least 2 min.
5. Repeat **steps 1–4** for other devices on the chip.

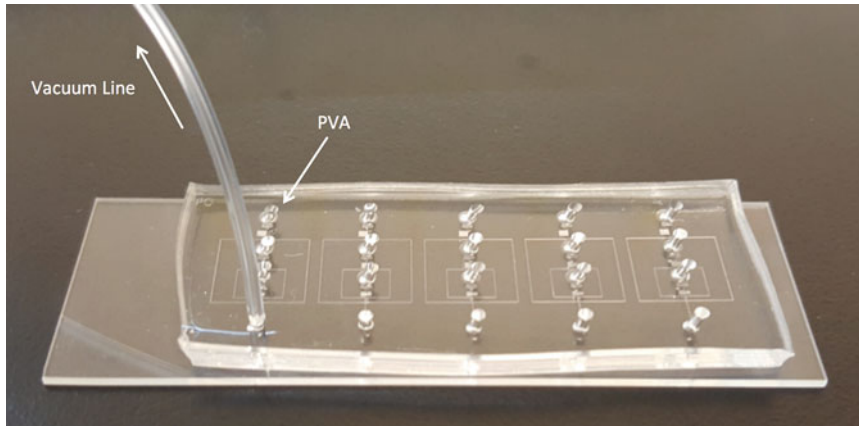

Fig. 5 Photograph of setup for PVA treatment. Place PVA solution at the inlet of the external phase channel with the vacuum applied to the outlet

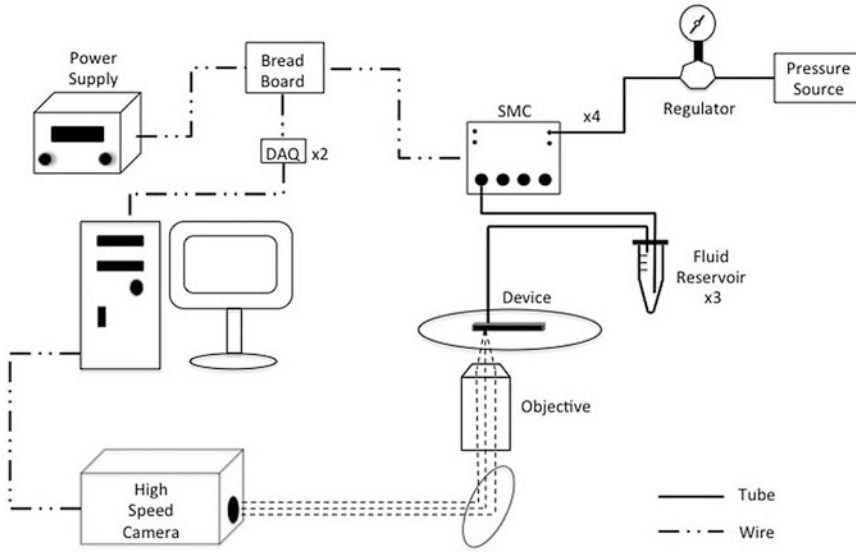

Fig. 6 Schematic diagram of experimental setup

6. Place the device in a 120 °C oven for at least 12 h.
7. Devices can be stored at room temperature in a dry environment for up to a year before use.

Generally, five devices are prepared at a given time so that backup devices are ready in case a leak or other imperfection prevents proper functioning during an experiment. Devices can also be made in bulk and kept in reserve for later use (approx. 6–12 months). Five devices can take approximately 30 min to bond and surface treat, and given the PDMS curing time of 4 h, up to 30 devices can be fabricated in a single working day.

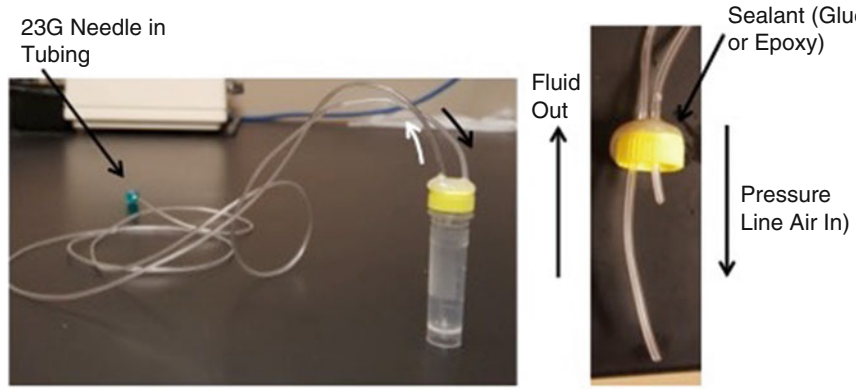

Fig. 7 Image of fluid reservoir tube

3.4 Double Emulsion Production

Experimental Setup.

A schematic of the experimental setup is shown in Fig. 6. The device is viewed on an inverted microscope via a high-speed camera connected to the side port, and the pressure of the inlet fluids is controlled via an SMC pressure regulator. The regulator obtains air from a house air source, and is controlled via a Labview VI. Two DAQs are used to interface the LabVIEW VI with the four pressure lines of the SMC regulator. The input line of the fluid reservoirs (Fig. 7) are connected to one of the four available pressure lines, with the output line inserted into the appropriate channel of the device.

1. Connect internal, oil, and external phase solutions to proper inlets in device (refer to Fig. 1). Tubing of fluid reservoirs (Fig. 7) should be primed before connection to device.
2. Connect the pressure lines of the fluid reservoirs to the pressure lines of the SMC regulators.
3. Run a pressure of 2 psi to each line until all fluids meet at the droplet generation junction.
4. Lower the pressure of the oil line to 1.5 psi, and lower the internal phase line to 0.5 psi or until it retreats from the droplet formation region.
5. Increase the pressure of the internal phase line slightly to reintroduce it to the droplet formation region, sheathed by the oil phase and not interacting with the walls of the device (Fig. 8).
6. Varying the internal phase pressure allows larger variations in droplet diameter while variations in the external phase pressure allow for more subtle variations (Fig. 9). Shell size variations and multiple internal droplets can be achieved by further increasing the oil phase pressure (data not shown).

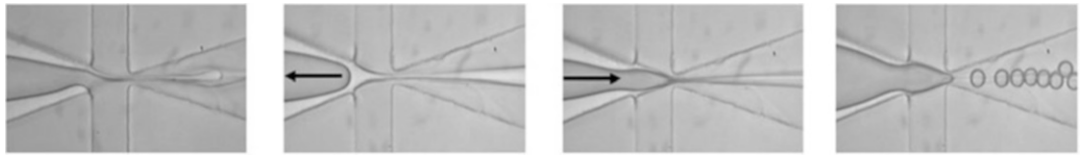

Fig. 8 Correction procedure for wetting of internal phase. (*Left-to-right*) Image of internal phase breaking through oil phase, decrease internal phase pressure, reintroduce internal phase, and droplet production reinitiates

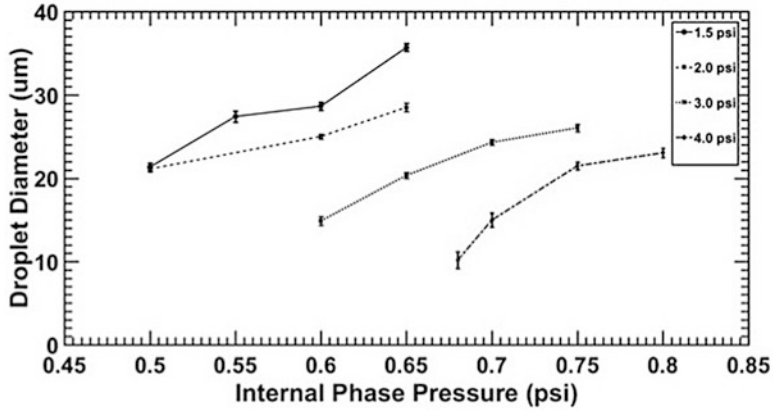

Fig. 9 Characterization of device using a pressure source for each fluid phase. Values in the legend represent the pressure of the external phase. The pressure of the oil phase was varied from 0.8–1.0 psi to maintain stable double emulsion production

Table 1
Size distribution for select double emulsion diameters

Intended diameter (μm)	Actual diameter (μm)
10	9.0 ± 0.6
15	14.9 ± 0.5
20	21.4 ± 0.5
30	30.9 ± 0.6

Table 2
Double emulsion population count over the course of 8 months in storage solution at room temperature. ($p = 0.0926$, 1-way ANOVA)

Time (months)	Concentration (particles/ml) $\times 10^6$
0	1.42 ± 0.10
2	1.37 ± 0.06
4	1.32 ± 0.09
8	1.27 ± 0.16

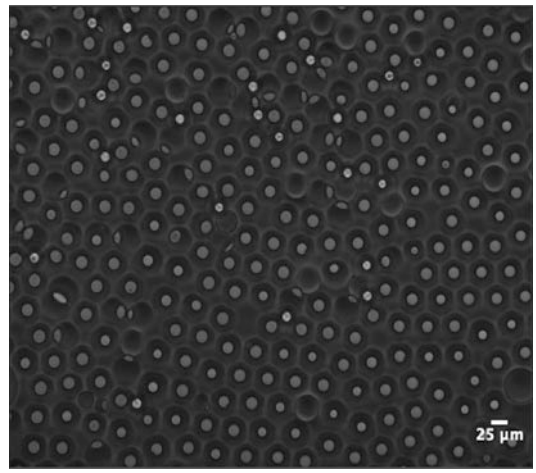

Fig. 10 Phase contrast image of a population of vesicles after dewetting. The *bright structures* within or to the side of the larger round structures (vesicles) are the oil "caps"

7. Collect and store double emulsions in excess storage solution (method 1) or excess external solution (method 2) at room temperature.
8. The double emulsions are highly monodisperse (Table 1) and can be stored for at least 8 months (Table 2).

3.5 Formation of Vesicles

3.5.1 Method 1

(a) To form the vesicles, dilute the double emulsion solution in PBS at a 1:5 ratio or greater. Double emulsions should begin to form lipid vesicles within 1 min (Fig. 10).

3.5.2 Method 2

(a) Store the double emulsions in excess external solution (14% ETOH) to extract the oleic acid from the double emulsion shell.

(b) The extraction process will take approximately 15 h. Leave the double emulsions at room temperature overnight. Please refer to [49] for further information on this process.

During production, components of a biosensing reaction can be encapsulated within the double emulsion, while membrane proteins or pores can be introduced once the vesicles are formed through nano-vesicle fusion techniques [52, 53]. Membrane components that spontaneously insert into lipid bilayers can simply be placed in solution with the fully formed vesicles or included within the internal phase during double emulsion production.

3.6 Insert Membrane Protein Pore

1. Use a 7:3 molar ratio of DOPC:DOPG (1,2-dioleoyl-sn-glycero-3-phospho-(1′-rac-glycerol), Avanti Polar Lipids) in the middle solution (Subheading 2.5, **item 2**) to generate the

vesicles. Include 100 μM of the pH sensitive fluorescent probe fluorescein (Fluka, MW = 33.32) in internal phase to verify pore formation.

2. Following dewetting in PBS, mix with 4.5 μM melittin in PBS and incubate for 30 min. A subset of the vesicle population should act as a control, and should not be exposed to melittin.

Melittin, the major toxin found in bee venom, is an antimicrobial peptide that forms nonspecific pores in lipid bilayers [54]. Since vesicles are able to encapsulate a large variety of species that can be used in biosensors, such as ions, small organic molecules, biological macromolecules, and nanoparticles, pore-forming toxins can create a pore to let analyte(s) permeate into the vesicles for detection [55]. α-hemolysin (αHL), a bacterial pore-forming toxin, is another popular choices due to its self-assembling capability to form 1.4 nm transbilayer channels [56].

Melittin insertion can be verified via a pH sensitive fluorescent dye. The internal phase of the vesicles do not include any buffer, making the interior slightly acidic. Fluorescein demonstrates weak fluorescence in acidic solutions, but fluoresces brightly when the pH = 7. When melittin inserts into the bilayer, PBS is allowed to enter and neutralize the vesicle interior, resulting in increased brightness. After 30 min of incubation in our test, the control sample had a mean pixel intensity of $(8.6 \pm 1.9) \times 10^5$ a.u (arbitrary units) while the sample exposed to melittin showed a mean pixel intensity of $(25 \pm 5.3) \times 10^5$ a.u. ($p < 0.01$, $N = 16$, Student T-Test).

3.7 Integration of Sensing Element onto Vesicles

3.7.1 Method 1 (Covalently Bonded Amine Reaction)

(a) Prepare the vesicles using a 10% molar ratio of DSPE-PEG (2000) Cyanur (Avanti Polar Lipids) to DOPC in the middle solution (Subheading 2.5, **item 2**) according to the steps in Subheading 3.4.

(b) Disperse vesicles into phosphate buffer (40 mM, pH 8.3) and add 0.2 M protein for overnight.

(c) Wash with PBS three times to remove unbound protein.

Proteins are covalently coupled to the vesicles via amine-reactive cyanur-groups, either directly to the vesicle surface using cyanuric chloride-activated DSPE (cyanur-DSPE) or to the distal ends of PEG-spacers using activated cyanur-PEG_{2000}-PE(Cyanur 1,2-distearoyl-sn-glycero-3-phosphoethanolamine-*N*-[cyanur (polyethylene glycol)-2000] (ammonium salt)) (Fig. 11) [57, 58]. Cyanuric chloride at the PEG terminus functions to link peptides, antibodies and other amine-containing biomolecules or nanoparticles via a nucleophilic substitution reaction under basic conditions. Antibodies or other proteins can be conjugated without any previous derivatization. In this study, we used fluorescent IgG-FITC (Jackson ImmunoResearch) as a model protein to ensure successful conjugation (Fig. 12). For sensing purposes, the protein or

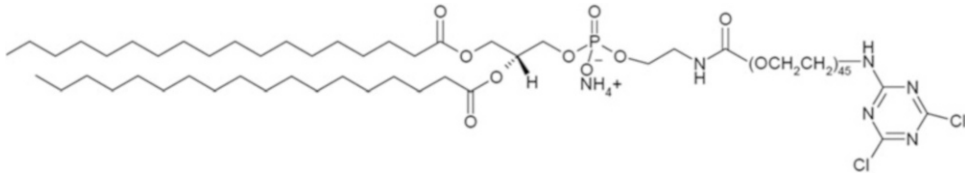

Fig. 11 Structure of DSPE-PEG(2000) Cyanur

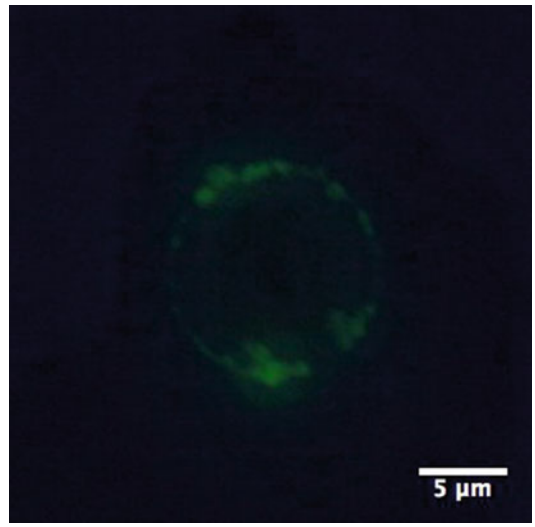

Fig. 12 Image of the vesicle conjugated with IgG-FITC

antibody orientation can also be an important issue. If the N-terminus of an antibody is correlated with the binding part of antigen [59], Protein A (Sigma-Aldrich) could be used to ensure proper orientation, as it specifically binds with the Fc domain of antibodies, leaving the antigen binding region exposed and facing away from the vesicle surface for optimal antigen capture [35].

3.7.2 Method 2 (Biotin–Avidin Interaction)

(a) Prepare the vesicles using a 1–10% molar ratio biotinylated lipid (DSPE-PEG(2000) Biotin, Avanti Polar Lipids) to DOPC in the middle solution (Subheading 2.5, **item 2**) according to the steps in Subheading 3.4. Add avidin and the biotinylated protein/antibody into PBS at a molar ratio determined by the number of binding sites you wish to occupy on the avidin. Since one binding site on the avidin will be used to attach to the vesicle surface, the ratio of avidin to available binding sites should be 1:1. The molar ratio of avidin to biotinylated antibody can vary from 1:1, 1:2, or 1:3. Incubate the mixture at room temperature for 15 min. Equation 1 can be used to estimate the moles of avidin required (DOPC Headgroup Area ≈ 72 Å^2 [60]):

$$\text{Moles Avidin} = \frac{\text{Vesicle Surface Area}}{(\text{Lipid Headgroup Area}) \times N_A} \times (\text{Molar Fraction Biotinylated Lipid}) \times (\text{Vesicle Concentration}) \times (\text{Vesicle Solution Volume})$$

N_A: Avagadro's Number

Eq. 1 Estimation of moles of avidin to add to biotinylated vesicle solution

(b) Disperse vesicles into the PBS solution used in **step 2**.

(c) Wash with PBS three times to remove unbound protein/antibodies.

The biotin–avidin interaction is high affinity, irreversible [61, 62], and has been demonstrated successfully to functionalized vesicle membranes and lipid surfaces [63–65]. Labeling proteins with biotin and using biotinylated lipids can link these two components irreversibly with avidin in a sandwiched structure. With the biotin–avidin interaction, antibodies with a biotinylated Fc domain can be conjugated to the vesicle membrane with the binding site oriented away from the surface.

4 Notes

1. The ability to encapsulate a high concentration of signaling molecules into vesicles via microfluidic droplet production is also advantageous to amplify binding events in an immunoassay. For example, Damhorst et al. [35] demonstrated the use of vesicles as proof-of-concept ion-release vehicles for an impedance sensor to measure HIV viral load in spiked samples of a lower conductivity buffer solution. To accomplish this, a PDMS flow-through device is bonded on a glass slide with integrated gold electrodes. Anti-gp120, which binds to gp120 on the HIV envelope, is immobilized to the surface of the microfluidic device, and caught HIV particles as they flowed through. After washing, anti-gp120 functionalized vesicles encapsulated with 10× PBS are passed through the device and bind to the viral particles in a sandwiched fashion. Heating the mixture lysed the vesicles and released the encapsulated ions, dramatically decreasing the impedance of the solution. The normalized impedance change in solution after 200 s, and the maximum change in impedance within that time, can both correlated to vesicle concentration, which in turn could theoretically be used to quantify viral load. The biorecognition element could also easily be changed to detect a variety of different analytes or pathogens.

Improved correlation between impedance change and vesicle concentration can be achieved by using a homogeneous vesicle population and more efficient encapsulation methods, which are not possible using standard bulk methods of vesicle generation [49]. Employing microfluidic methods of vesicle generation can help further improve this assay by ensuring consistent ion release from each vesicle. Alternative assays that utilize different types of reporter molecules and biorecognition elements [36–40] could also benefit from the monodispersity and encapsulation efficiency of microfluidic droplet production. Furthermore, many laboratories and institutions that specialize in such assays, are not proficient in the microfluidic production of vesicles, and would need them shipped from a source that could produce them. Given the short-shelf life of cell-sized vesicles, much of the population may be lost during shipment or compromised if the vesicles are freeze dried. With the method presented here, the highly stable double emulsions can be converted to vesicles upon arrival to their destination or ordered in bulk and stored until ready for use so that investigators have a steady supply of homogenous vesicles.

2. The utility of the described vesicle production method is the high encapsulation efficiency, monodispersity, and long-shelf life. A large concentration of a signal marker, such as ions or fluorescent molecules, or enzymatic reaction components, can be encapsulated in the double emulsions during production. When ready for use, the double emulsions can be converted into vesicles and have their surface functionalized with a biorecognition element or have a protein channel inserted in the membrane to allow access to internal reaction components. For example, Vamvakaki et al. [1] devised an elegant detection scheme to measure very small amounts (10−10 M) of the organophosphorus pesticides dichlorvos and paraoxon using vesicle biosensors that contained encapsulated acetylcholinesterase (AChE) and the membrane protein channel OmpF porin (Protein F). Protein F is a channel forming protein naturally found in E. coli that allows nonspecific passage of small molecules (<600 Da) through the membrane [66]. AChE works by hydrolyzing acetylcholine that has entered the vesicle interior via the Protein F channels, producing choline and acetic acid. Acetic acid decreases the pH in the vesicle interior, which is monitored with the co-encapsulation of the pH sensitive fluorescent dye pyranine. Pyranine fluoresces brightly at low pH, and dims as the pH approaches neutral. Pesticides present in a sample pass through Protein F channels into the vesicle interior and irreversibly inhibit the activity of AChE, discouraging a drop in pH and resulting in a lower signal. The intensity of the fluorescent signal is correlated to the concentration of pesticide in solution, from a range

of 10−4 – 10−12 M. The detection range is promising for measuring the amount pesticides present in contaminated drinking water.

Acknowledgments

This work was funded in part by the National Institute of Health, Grant No. R01-EB012058.

References

1. Vamvakaki V, Chaniotakis NA (2007) Pesticide detection with a liposome-based nanobiosensor. Biosens Bioelectron 22:2848–2853
2. Peterson RD, Chen WL, Cunningham BT, Andrade JE (2015) Enhanced sandwich immunoassay using antibody-functionalized magnetic iron-oxide nanoparticles for extraction and detection of soluble transferrin receptor on a photonic crystal biosensor. Biosens Bioelectron 74:815–822
3. Bhuvana M, Narayanan JS, Dharuman V, Teng W, Hahn JH, Jayakumar K (2013) Gold surface supported spherical liposome-gold nanoparticle nano-composite for label free DNA sensing. Biosens Bioelectron 41:802–808
4. Zou L, Wang Q, Tong MM, Li HB, Wang J, Hu N et al (2016) Detection of diarrhetic shellfish poisoning toxins using high-sensitivity human cancer cell-based impedance biosensor. Sensors and Actuators B-Chemical 222:205–212
5. Solovyev A, Kuncova G, Demnerova K (2015) Whole-cell optical biosensor for mercury – operational conditions in saline water. Chem Papers 69:183–191
6. Girousi ST, Pantazaki AA, Voulgaropoulos AN (2001) Mitochondria-based amperometric biosensor for the determination of L-glutamic acid. Electroanalysis 13:243–245
7. Carpentier R, Loranger C, Chartrand J, Purcell M (1991) Photoelectrochemical cell containing chloroplast membranes as a biosensor for phytotoxicity measurements. Anal Chim Acta 249:55–60
8. Yun YH, Eteshola E, Bhattacharya A, Dong ZY, Shim JS, Conforti L et al (2009) Tiny medicine: nanomaterial-based biosensors. Sensors 9:9275–9299
9. Kim HJ, Bennetto HP, Halablab MA (1995) A novel liposome-based electrochemical biosensor for the detection of hemolytic microorganisms. Biotechnol Techniques 9:389–394
10. Zehani N, Fortgang P, Lachgar MS, Baraket A, Arab M, Dzyadevych SV et al (2015) Highly sensitive electrochemical biosensor for bisphenol A detection based on a diazonium-functionalized boron-doped diamond electrode modified with a multi-walled carbon nanotube-tyrosinase hybrid film. Biosens Bioelectron 74:830–835
11. Li DD, Cheng W, Yan YR, Zhang Y, Yin YB, Ju HX et al (2016) A colorimetric biosensor for detection of attomolar microRNA with a functional nucleic acid-based amplification machine. Talanta 146:470–476
12. Bhand SG, Soundararajan S, Surugiu-Warnmark I, Milea JS, Dey ES, Yakovleva M et al (2010) Fructose-selective calorimetric biosensor in flow injection analysis. Anal Chim Acta 668:13–18
13. Park SC, Cho EJ, Moon SY, Yoon SI, Kim YJ, Kim DH et al (2007) A calorimetric biosensor and its application for detecting a cancer cell with optical imaging. World Congress on Medical Physics and Biomedical Engineering 2006, Vol 14, Pts 1–6 14:637–640
14. Jang H, Jung S, Shin KS, Kim SM, Jeon TJ (2014) Polydiacetylene (PDA) vesicle based colorimetric biosensor for detection of genetically modified (GM) crops. Biophys J 106:417a–417a
15. Giamblanco N, Conoci S, Russo D, Marletta G (2015) Single-step label-free hepatitis B virus detection by a piezoelectric biosensor. Rsc Adv 5:38152–38158
16. Kim S, Choi SJ (2014) A lipid-based method for the preparation of a piezoelectric DNA biosensor. Anal Biochem 458:1–3
17. Bahadir EB, Sezginturk MK (2015) Applications of commercial biosensors in clinical, food, environmental, and biothreat/biowarfare analyses. Anal Biochem 478:107–120
18. Justino CIL, Freitas AC, Pereira R, Duarte AC, Santos TAPR (2015) Recent developments in

recognition elements for chemical sensors and biosensors. Trac-Trends Anal Chem 68:2–17

19. Vamakaki V, Chaniotakis NA (2007) Carbon nanostructures as transducers in biosensors. Sens Actuat B Chem 126:193–197
20. Frey S, Millat T, Hohmann S, Wolkenhauer O (2008) How quantitative measures unravel design principles in multi-stage phosphorylation cascades. J Theor Biol 254:27–36
21. Eriksson E, Aspan A (2007) Comparison of culture, ELISA and PCR techniques for salmonella detection in faecal samples for cattle, pig and poultry. BMC Vet Res 3:21
22. Mello LD, Kubota LT (2002) Review of the use of biosensors as analytical tools in the food and drink industries. Food Chem 77:237–256
23. van den Hurk R, Evoy S (2015) A Review of Membrane-Based Biosensors for Pathogen Detection. Sensors 15:14045–14078
24. Jin LY, Dong YM, Wu XM, Cao GX, Wang GL (2015) Versatile and amplified biosensing through enzymatic cascade reaction by coupling alkaline phosphatase in situ generation of photoresponsive nanozyme. Anal Chem 87:10429–10436
25. Zhu X, Sun L, Chen YY, Ye ZH, Shen ZM, Li GX (2013) Combination of cascade chemical reactions with graphene-DNA interaction to develop new strategy for biosensor fabrication. Biosens Bioelectron 47:32–37
26. Kuiper SM, Nallani M, Vriezema DM, Cornelissen JJLM, van Hest JCM, Nolte RJM et al (2008) Enzymes containing porous polymersomes as nano reaction vessels for cascade reactions. Org Biomol Chem 6:4315–4318
27. van Dongen SFM, Nallani M, Cornelissen JLLM, Nolte RJM, van Hest JCM (2009) A three-enzyme cascade reaction through positional assembly of enzymes in a polymersome nanoreactor. Chem A Eur J 15:1107–1114
28. Tanner P, Balasubramanian V, Palivan CG (2013) Aiding nature's organelles: artificial peroxisomes play their role. Nano Lett 13:2875–2883
29. Ben-Haim N, Broz P, Marsch S, Meier W, Hunziker P (2008) Cell-specific integration of artificial organelles based on functionalized polymer vesicles. Nano Lett 8:1368–1373
30. Steller L, Kreir M, Salzer R (2012) Natural and artificial ion channels for biosensing platforms. Anal Bioanal Chem 402:209–230
31. Reppy MA, Pindzola BA (2007) Biosensing with polydiacetylene materials: structures, optical properties and applications. Chem Commun 42:4317–4338
32. Silbert L, Ben Shlush I, Israel E, Porgador A, Kolusheva S, Jelinek R (2006) Rapid chromatic detection of bacteria by use of a new biomimetic polymer sensor. Appl Environ Microbiol 72:7339–7344
33. Su YL, Li JR, Jiang L (2005) A study on the interactions of surfactants with phospholipid/polydiacetylene vesicles in aqueous solutions. Colloids Surf A Physicochem Eng Aspects 257–58:25–30
34. Bally M, Bailey K, Sugihara K, Grieshaber D, Voros J, Stadler B (2010) Liposome and lipid bilayer arrays towards biosensing applications. Small 6:2481–2497
35. Damhorst GL, Smith CE, Salm EM, Sobieraj MM, Ni HK, Kong H et al (2013) A liposome-based ion release impedance sensor for biological detection. Biomed Microdevices 15:895–905
36. Ho JAA, Wauchope RD (2002) A strip liposome immunoassay for aflatoxin B-1. Anal Chem 74:1493–1496
37. Ahn-Yoon S, DeCory TR, Durst RA (2004) Ganglioside-liposome immunoassay for the detection of botulinum toxin. Anal Bioanal Chem 378:68–75
38. Ho JAA, Zeng SC, Tseng WH, Lin YJ, Chen CH (2008) Liposome-based immunostrip for the rapid detection of Salmonella. Anal Bioanal Chem 391:479–485
39. Rongen HAH, Vanderhorst HM, Hugenholtz GWK, Bult A, Vanbennekom WP, Vandermeide PH (1994) Development of a liposome immunosorbent-assay for human interferon-gamma. Anal Chim Acta 287:191–199
40. Ou LJ, Liu SJ, Chu X, Shen GL, Yu RQ (2009) DNA encapsulating liposome based rolling circle amplification immunoassay as a versatile platform for ultrasensitive detection of protein. Anal Chem 81:9664–9673
41. Chen H, Zheng Y, Jiang JH, Wu HL, Shen GL, Yu RQ (2008) An ultrasensitive chemiluminescence biosensor for cholera toxin based on ganglioside-functionalized supported lipid membrane and liposome. Biosens Bioelectron 24:684–689
42. Cooper MA, Hansson A, Lofas S, Williams DH (2000) A vesicle capture sensor chip for kinetic analysis of interactions with membrane-bound receptors. Anal Biochem 277:196–205
43. Patolsky F, Lichtenstein A, Willner I (2000) Amplified microgravimetric quartz-crystal-microbalance assay of DNA using oligonucleotide-functionalized liposomes or biotinylated liposomes. J Am Chem Soc 122:418–419
44. Grieshaber D, de Lange V, Hirt T, Lu Z, Voros J (2008) Vesicles for signal amplification in a biosensor for the detection of low antigen concentrations. Sensors 8:7894–7903

45. Liu QT, Boyd BJ (2013) Liposomes in biosensors. Analyst 138:391–409
46. Teh SY, Lin R, Hung LH, Lee AP (2008) Droplet microfluidics. Lab Chip 8:198–220
47. Shum HC, Lee D, Yoon I, Kodger T, Weitz DA (2008) Double emulsion templated monodisperse phospholipid vesicles. Langmuir 24:7651–7653
48. Hayward RC, Utada AS, Dan N, Weitz DA (2006) Dewetting instability during the formation of polymersomes from block-copolymer-stabilized double emulsions. Langmuir 22:4457–4461
49. Teh S-Y, Khnouf R, Fan H, Lee AP (2011) Stable, biocompatible lipid vesicle generation by solvent extraction-based droplet microfluidics. Biomicrofluidics 5:044113–044113-12
50. Duffy DC, McDonald JC, Schueller OJA, Whitesides GM (1998) Rapid prototyping of microfluidic systems in poly(dimethylsiloxane). Anal Chem 70:4974–4984
51. Xia YN, Whitesides GM (1998) Soft lithography. Angew Chem Int Ed 37:551–575
52. K. Tsumoto, K. Kamiya, S. Kitaoka, S. Ogata, M. Tomita, and T. Yoshimura(2009) G protein coupled receptors (GPCRs) reconstituted on recombinant proteoliposomes using baculovirus-liposome membrane fusion. In: Micro-nanomechatronics and human science. International Symposium on MHS 2009. 2009: 202–207.
53. Csiszár A, Hersch N, Dieluweit S, Biehl R, Merkel R, Hoffmann B (2010) Novel fusogenic liposomes for fluorescent cell labeling and membrane modification. Bioconjug Chem 21:537–543
54. Lee MT, Sun TL, Hung WC, Huang HW (2013) Process of inducing pores in membranes by melittin. Proc Natl Acad Sci U S A 110:14243–14248
55. Hsin TM, Wu K, Chellappan G (2012) Magnetically immobilized nanoporous giant proteoliposomes as a platform for biosensing. Analyst 137:245–248
56. Lemiere J, Guevorkian K, Campillo C, Sykes C, Betz T (2013) alpha-Hemolysin membrane pore density measured on liposomes. Soft Matter 9:3181–3187
57. Bakowsky H, Richter T, Kneuer C, Hoekstra D, Rothe U, Bendas G et al (2008) Adhesion characteristics and stability assessment of lectin-modified liposomes for site-specific drug delivery. BBA-Biomembranes 1778:242–249
58. Bendas G, Krause A, Bakowsky U, Vogel J, Rothe U (1999) Targetability of novel immunoliposomes prepared by a new antibody conjugation technique. Int J Pharm 181:79–93
59. Baksh MM, Dean C, Pautot S, DeMaria S, Isacoff E, Groves JT (2005) Neuronal activation by GPI-linked neuroligin-1 displayed in synthetic lipid bilayer membranes. Langmuir 21:10693–10698
60. Kucerka N, Tristram-Nagle S, Nagle JF (2005) Structure of fully hydrated fluid phase lipid bilayers with monounsaturated chains. J Membr Biol 208:193–202
61. Wilchek M, Bayer EA (1990) Introduction to avidin-biotin technology. Methods Enzymol 184:5–13
62. Guesdon JL, Ternynck T, Avrameas S (1979) Use of avidin-biotin interaction in immunoenzymatic techniques. J Histochem Cytochem 27:1131–1139
63. Giannoni F, Barnett J, Bi K, Samodal R, Lanza P, Marchese P et al (2005) Clustering of T cell Ligands on artificial APC membranes influences T cell activation and protein kinase C theta translocation to the T cell plasma membrane. J Immunol 174:3204–3211
64. Zappasodi R, Di Nicola M, Carlo-Stella C, Mortarini R, Molla A, Vegetti C et al (2008) The effect of artificial antigen-presenting cells with preclustered anti-CD28/−CD3/−LFA-1 monoclonal antibodies on the induction of ex vivo expansion of functional human antitumor T cells. Haematologica 93:1523–1534
65. Hettiarachchi K, Lee AP, Zhang S, Feingold S, Dayton PA (2009) Controllable microfluidic synthesis of multiphase drug-carrying lipospheres for site-targeted therapy. Biotechnol Prog 25:938–945
66. Koebnik R, Locher KP, Van Gelder P (2000) Structure and function of bacterial outer membrane proteins: barrels in a nutshell. Mol Microbiol 37:239–253